ACADEMIA ROMÂNĂ
Revue Roumaine de Chimie
http://web.icf.ro/rrch/

Rev. Roum. Chim.,
2011, *56*(12), 1119-1127

THERMODYNAMIC AND STRUCTURAL PROPERTIES OF PENETRABLE-SPHERE SYSTEMS: THEORY AND SIMULATION**

Viorel CHIHAIA,[a] Jose Maria CALDERON-MORENO,[a] Nicolae STANICĂ,[a]
Viorica PARVULESCU,[a] Mariuca GARTNER[a] and Soong-Hyuck SUH[b]*

[a] "I.G. Murgulescu" Institute of Physical Chemistry, Roumanian Academy, 202 Splaiul Independentei, Bucharest 060021, Roumania
[b] Department of Chemical Engineering, Keimyung University, Daegu 704-701, Korea

Received December15, 2010

Computer simulations via the molecular dynamics method have been carried out to investigate the thermodynamic and structural properties of penetrable-sphere interaction systems over the wide ranges of the packing fraction, φ , and the repulsive energy parameter, ε^* . The resulting molecular dynamics simulation data for the configurational energy, the compressibility factor and the contact value of the radial distribution function are used to assess the applicabilities of various theoretical predictions available in the literature including high- and low-penetrability approximations. A reasonable agreement between theoretical and simulation results is found in the cases of low and moderately repulsive systems ($\varepsilon^* \leq$ 1.0). However, for dense systems of $\varphi \geq$ 0.6 with the highly repulsive energy barrier of ε^* = 3.0, a poor agreement is observed due to the metastable static effects of cluster-forming structures in the phase transition state.

INTRODUCTION

During the last couple of decades much progress has been made in our understanding of thermodynamic and related structural properties of soft-condensed matter including colloids, polymers, foams, gels, granular materials, and a number of biological materials. The effective model potentials can be of various nature,[1] and the different minimal model has to be considered accounting for the boundness of repulsive interactions in such soft-condensed systems. One of simplest model systems in this approach is the so-called penetrable-sphere (PS) model system, in which two overlapping spheres can penetrate each other with the finite repulsive energy parameter. This bounded PS potential has been the subject of several theoretical and simulation studies.[2-11] More recently, the PS model potential has been extended to include a short-range attractive tail.[12-14]

Reliable and unambiguous results, in turn, have become increasingly necessary to eliminate any underlying uncertainties involved in theoretical approximations. The classical integral equation theories[15] do not describe satisfactorily well the structure of the PS fluid, especially inside the overlapping core-region for low temperatures. From this theoretical point of view, the PS model can be used as a stringent benchmark to test alternative statistical thermodynamic approximations, and the derivation of exact properties provides an invaluable tool. From the experimental point of view, on the other hand, the present level of modeling, particularly under the meso- or macroscopic continuum assumption, is far too crude to allow the direct comparison with real experiments. Consequently, molecular-based

* Corresponding author: shsuh@kmu.ac.kr
** Dedicated to Dr. Vlad T. Popa for his special contributions as a co-organizer in the Korea/Roumania Joint Workshop

computer simulations, which provide essentially exact machine data for precisely defined model systems, have proven to be an extremely useful diagnostic tool.[16]

One of the authors[17] has investigated two different theoretical predictions, based on the fundamental-measure theory proposed by Schmidt[4] and the bridge density-functional approximation proposed by Zhou and Ruckenstein,[18] to the inhomogeneous structure of PS model fluids in the spherical pore system. As a continuation of theoretical and simulation approaches along this direction,[19] the modified density-functional theory (based on both the bridge density functional and the contact-value theorem) has been applied to the structural properties of PS fluids near a slit hard wall, and the Verlet-modified bridge function for one-component systems proposed by Choudhury and Ghosh[7] has also been extended to PS fluid mixtures. Very recently, in addition to equilibrium static properties of such bounded potentials, simulation studies for time-dependent dynamic properties have been reported to add useful insights into the cluster formation and diffusion behavior of the PS model fluid.[20]

There are in general two classes of computer simulation approaches: stochastic Monte Carlo (MC) and deterministic molecular dynamics (MD) methods. In MD calculations, the actual trajectories of atoms or molecules are evaluated by the numerical integration of Newton's equations of motion, in which time-dependent transport properties can be determined. Up to the date, almost all simulations for the PS model fluid have been carried out using the MC method. Computationally, a better statistics can be achieved in MD simulations in system with discontinuous interactions. For instance, in order to calculate the virial route to the equation of state for hard-core systems, MC computations require an accurate estimation of the pair distribution function. In many cases the pair distribution function may change rapidly near the contact distance in the systems of ionic solutions, highly charged colloids, aligned liquid crystals, etc. Under those conditions the extrapolation to the contact value often lead to large uncertainties.[21,22] For this reason, the pressure determined by MC calculations is known to be less accurate than that by MD simulations.

The main motivation in the present work is to undertake the MD simulation study of thermodynamic and structural properties for the system of PS model fluids over a wide range of densities and repulsive energy parameters, which can be directly compared with various statistical mechanical predictions available in the literature. Together with existing theoretical approximations for the equilibrium equation of state, our simulation result can be used to construct a fundamental basis of theoretical and practical predictions for the equilibrium and related structural properties. Such simulation approaches at the atomic or molecular level can also be used to improve statistical integral-equation theories of liquid state, and also to help in interpreting the real experimental data.

MODEL AND SIMULATIONS

The penetrable-sphere potential is defined as a function of the relative distance, r, between pair particles i and j,

$$u_{ij}(r) = \begin{cases} \varepsilon, & r \le \sigma \\ 0, & r > \sigma, \end{cases} \tag{1}$$

where σ is the diameter of the penetrable spheres, and ε (>0) is the strength of the repulsive energy barrier when two PS particles penetrate each other. The PS interaction model reduces to the classical hard-sphere (HS) system when ε^* (= ε/kT)→ ∞ where k is the Boltzmann constant and T is the temperature. This is equivalent to the zero-temperature limit T^* (= kT/ε)→ 0 . In the opposite high-penetrability or high-temperature limit ($\varepsilon^* \to 0$ or $T^* \to \infty$), the PS system becomes a collisionless ideal gas. In the PS system the overlapping penetrability allows one in principle to consider any value of the nominal packing fraction, φ (= $(\pi/6)\rho\sigma^3$) , where ρ (= N/V) is the particle number density, N, the number of particles, and V, the system volume. Note that the maximum packing fraction in the pure HS system is about 0.74 from the face-centered cubic structure.

As a successful diagnostics tool, computer simulations are usually employed to investigate the underlying static and dynamic behavior of the model potential system of interest. To this end, we have carried out microcanonical MD simulations for the PS model fluid in a manner similar to that originally proposed by Alder and Wainwright for hard-core systems.[23] Post-collision velocities for

colliding pairs of PS particles were assigned according to the type of collisions: either hard-type specular reflection or soft-type refraction. In both collision conditions the total momentum and kinetic energies are conserved in the PS system. Interestingly, in the PS binary collision dynamics the particle penetration is analogous to the double refraction of light through a sphere made of a transparent material of relative refraction index depending on the relative collision velocity and the repulsive energy parameter. A more detailed algorithm with the schematic collision diagram is also described elsewhere.[20,24]

The conventional periodic boundary conditions were applied in a cubic fundamental cell to approximate an infinite thermodynamic system. To assist the fast equilibration state in our MD simulations, the initial configurations with 864 penetrable spheres were generated by randomly inserting PS particles with velocities drawn from the Maxwell-Boltzmann distribution. The initial configurations were aged, or equilibrated, for 5×10^6 collisions before accumulating the final simulation results. Additional ensemble averages were evaluated from a total number of 5×10^8 collisions. Our MD algorithm employed in this work has been tested in a number of ways. When the repulsive energy parameter was assigned to large values (typically, $\varepsilon^* > 3$) at the low-density regime (typically, $\varphi < 0.2$), the static and dynamic results generated from our MD simulations faithfully reproduced the pure HS system. Our resulting MD calculations for a few selected runs were also compared with MC computations reported in the literature.[11] An excellent agreement with previous MC data for the thermodynamic and structural properties again confirmed the validity of the MD method employed in this work. All MD results reported here are scaled to dimensionless quantities by using a unit particle diameter σ, a unit particle mass m, and a unit thermal energy kT.

RESULTS AND DISCUSSION

System characteristics investigated in this work and MD simulation results for the reduced configurational energy, U/NkT, and the compressibility factor, Z (=PV/NkT), are presented in Table 1. The value in parentheses indicates the standard error in our MD simulations, which was estimated from 50 independent partial averages taken over the entire length in a given thermodynamic condition. In this table we also report the MD contact values of the radial distribution function, $g(\sigma^-)$ and $g(\sigma^+)$, together with theoretical predictions using the high-penetrability approximation (HPA), $g_{\mathrm{HPA}}(\sigma^+)$, and the low-penetrability approximation (LPA), $g_{\mathrm{LPA}}(\sigma^+)$.

In Fig. 1, we have displayed the reduced configurational energy, U/NkT, as a function of the packing fraction φ for the PS systems. Also shown in this figure is the theoretical approximation available in the literature.[7,17] The thermodynamic properties can be expressed in terms of the radial distribution function, $g(r)$. For the PS system, the reduced configurational energy is written as

$$\frac{U}{NkT} = 12\varphi\varepsilon^* \int_0^\sigma g(r)\, dr. \qquad (2)$$

The resulting MD value shows a good agreement with the theoretical predictions for the systems of low repulsive energy barriers ($\varepsilon^* = 0.2$), whereas very poor agreement is observed for the systems of the dense systems high ε-values ($\varepsilon^* = 3.0$) mainly due to the significant deteriorated structural effects inside the penetrable core-region. Moreover, in some cases of high density and high energy parameters ($\varphi \geq 0.6$ and $\varepsilon^* = 3.0$), these approximations generate unrealistic data with the negative value of the radial distribution function. It is worthwhile noting that enforcing the fulfillment of zero separation theorems and thermodynamic consistency conditions can lead to a reasonably good agreement with MC simulations for the thermodynamics as well as the structures inside and outside the PS particle core.[5] However, this requires additional parameter fittings and there is no guarantee to reach the global minimum for the residual inconsistencies.

Table 1

System characteristics and MD simulation results for penetrable-sphere model interactions.
The value in parentheses indicates the standard error in MD simulations over 50 independent partial averages

φ	U/NkT	$Z\ (=PV/NkT)$	$g(\sigma^-)$	$g(\sigma^+)$	$g_{\mathrm{HPA}}(\sigma^+)$	$g_{\mathrm{LPA}}(\sigma^+)$
$\varepsilon^* = 0.2$						
0.1	0.0662 (7.57×10^{-5})	1.073 (8.76×10^{-6})	0.8246	1.006	1.007	1.006
0.2	0.1338 (5.78×10^{-5})	1.147 (3.06×10^{-5})	0.8297	1.013	1.013	1.012
0.3	0.2024 (7.97×10^{-5})	1.222 (3.94×10^{-5})	0.8343	1.019	1.018	1.015
0.4	0.2719 (1.04×10^{-4})	1.297 (4.52×10^{-5})	0.8380	1.023	1.023	1.018
0.5	0.3421 (1.31×10^{-4})	1.373 (8.34×10^{-5})	0.8410	1.027	1.026	1.019
0.6	0.4131 (7.41×10^{-5})	1.449 (5.58×10^{-5})	0.8444	1.031	1.029	1.019
0.7	0.4845 (1.55×10^{-4})	1.525 (9.25×10^{-5})	0.8468	1.034	1.032	1.019
0.8	0.5563 (2.77×10^{-4})	1.602 (1.47×10^{-4})	0.8490	1.037	1.034	1.019
0.9	0.6285 (1.73×10^{-4})	1.679 (1.08×10^{-4})	0.8508	1.040	1.037	1.018
1.0	0.7012 (3.04×10^{-4})	1.756 (9.62×10^{-5})	0.8529	1.042	1.038	1.017
$\varepsilon^* = 1.0$						
0.1	0.1691 (5.81×10^{-4})	1.276 (3.54×10^{-4})	0.4015	1.091	1.071	1.092
0.2	0.3799 (1.03×10^{-3})	1.590 (4.89×10^{-4})	0.4290	1.161	1.112	1.167
0.3	0.6207 (1.96×10^{-3})	1.924 (9.10×10^{-4})	0.4469	1.212	1.137	1.223
0.4	0.8800 (2.98×10^{-3})	2.266 (1.46×10^{-3})	0.4584	1.247	1.154	1.262
0.5	1.1507 (3.00×10^{-3})	2.612 (1.48×10^{-3})	0.4663	1.270	1.165	1.288
0.6	1.4228 (2.57×10^{-3})	2.955 (1.19×10^{-3})	0.4690	1.286	1.173	1.301
0.7	1.7041 (5.81×10^{-3})	3.298 (3.06×10^{-3})	0.4747	1.293	1.179	1.305
0.8	1.9633 (4.37×10^{-3})	3.622 (2.94×10^{-3})	0.4693	1.301	1.183	1.299
0.9	2.2213 (8.11×10^{-3})	3.940 (5.59×10^{-3})	0.4660	1.303	1.185	1.286
1.0	2.4828 (6.81×10^{-3})	4.253 (5.05×10^{-3})	0.4666	1.294	1.186	1.267
$\varepsilon^* = 3.0$						
0.1	0.0875 (9.96×10^{-4})	1.479 (1.40×10^{-3})	0.06294	1.252	1.142	1.254
0.2	0.2702 (5.05×10^{-3})	2.189 (5.08×10^{-3})	0.07685	1.547	1.206	1.568
0.3	0.6238 (9.28×10^{-3})	3.074 (6.54×10^{-3})	0.08757	1.782	1.240	1.932
0.4	1.0965 (3.75×10^{-3})	3.902 (2.24×10^{-3})	0.08936	1.879	1.261	2.319
0.5	1.5726 (1.23×10^{-2})	4.603 (1.13×10^{-2})	0.09076	1.880	1.272	2.692
0.6	1.9379 (1.33×10^{-2})	5.139 (1.49×10^{-2})	0.08446	1.877	1.278	3.028
0.7	2.2641 (1.71×10^{-2})	5.554 (1.89×10^{-2})	0.07901	1.850	1.279	3.324
0.8	2.5269 (5.62×10^{-3})	5.815 (7.56×10^{-3})	0.06990	1.819	1.276	3.609
0.9	2.8080 (1.35×10^{-2})	6.063 (1.71×10^{-2})	0.06453	1.774	1.268	3.978
1.0	3.0282 (1.39×10^{-2})	6.218 (2.34×10^{-3})	0.05546	1.761	1.254	4.667

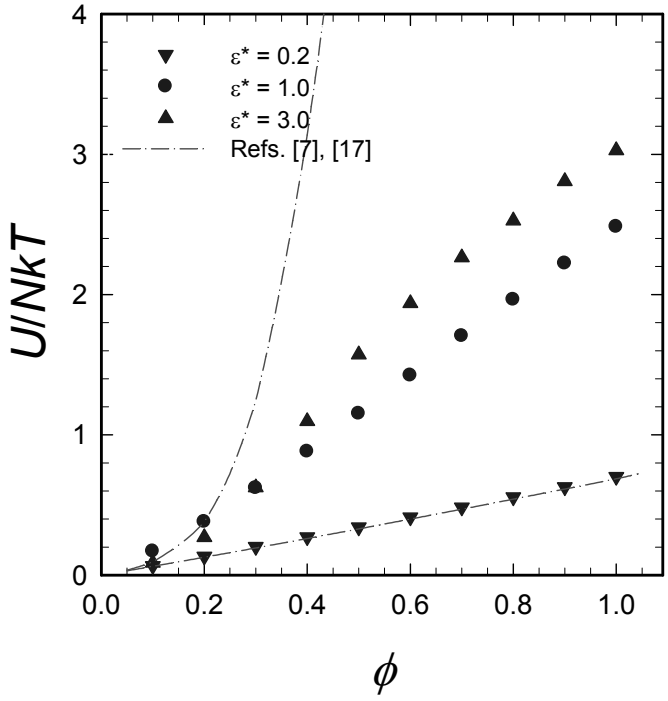

Fig. 1 – The reduced configurational energy as a function of packing fractions for the penetrable-sphere system. The symbols represent MD results, and the dash-dotted lines correspond to theoretical predictions in the literature[7,17] for ε^* = 0.2 and 3.0.

The compressibility factor, Z, of the HS system can be derived from the Carnahan-Starling (CS) equation of state with an excellent accuracy,[25]

$$Z^{CS} = \frac{1 + \varphi + \varphi^2 - \varphi^3}{(1-\varphi)^3}, \tag{3}$$

and, from the thermodynamic relation with the contact value in the radial distribution function, one may have

$$g^{CS}(\sigma^+) = \frac{Z^{CS} - 1}{4\varphi} = \frac{1 - \frac{\varphi}{2}}{(1-\varphi)^3}. \tag{4}$$

In the MD computations of discontinuous interaction systems including HS and PS models, the compressibility factor can be directly calculated using the Clausius theorem,[16]

$$Z = 1 + \frac{1}{3NkT}\frac{1}{t_{tot}}\sum_{coll} m\,\mathbf{r}_{ij}\cdot\Delta\mathbf{v}_{ij}, \tag{5}$$

where t_{tot} is the total elapsed simulation time over which the sum is evaluated, $\mathbf{r}_{ij}$ is the separation position vector, and $\Delta\mathbf{v}_{ij}$ is the instantaneous velocity change vector between colliding pair particles i and j. Alternatively, with the careful extrapolation of the radial distribution function to the contact point, the compressibility factor can be indirectly evaluated using the virial expression,[16] and, in the PS fluid, it is written as

$$Z = 1 + 4\varphi\,(1 - e^{-\varepsilon^*})\,g(\sigma^+). \tag{6}$$

The compressibility equation, or the equation of state, is often written as the simple linear polynomial equation in terms of the density or the packing fraction. Similarly, in this work the empirical PS compressibility approximation can be represented using up to the fourth order of φ,

$$Z = 1 + c_1\varphi + c_2\varphi^2 + c_3\varphi^3 + c_4\varphi^4 + O(\varphi^5). \tag{7}$$

In Fig. 2(a) and (b), we have illustrated the density dependence of the compressibility factor as a function of the packing fraction φ for the PS model systems. A good agreement between the two methods in Eqs. (5) and (6) is found for the systems of ε^*=0.2 and 1.0. For the dense systems ($\varphi \geq 0.6$) with the high repulsive parameter (ε^*=3.0), however, noticeable differences were detected in MD simulations. (We will return this point later in this section.) As displayed in these figures, the MD compressibility factor linearly increases with increasing densities for the most penetrable and moderately penetrable cases of ε^* = 0.2 and 1.0. Such a linear trend is no more realistic for the least penetrable case of ε^* = 3.0 even in the low density regime.

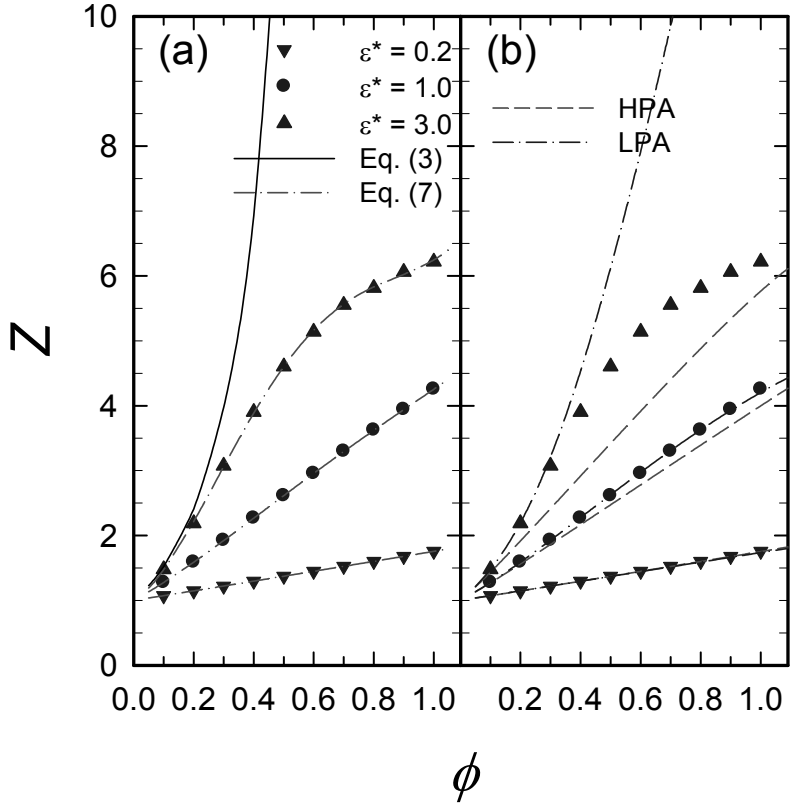

Fig. 2 – The compressibility factor as a function of packing fractions for the penetrable-sphere system. (a) The symbols represent MD results, and the single solid line and the dash-dotted lines, respectively, denote the Carnahan-Starling prediction in Eq. (3) for the hard-sphere fluid, and the least-square curve fitting data in Eq. (7) for the penetrable-sphere fluid. (b) The symbols represent MD results, and the dashed and the dash-dotted lines correspond to the high- and low-penetrability approximations, respectively.

In Fig. 2(a), only in the narrow density regime of $\varphi \leq$ 0.2 for $\varepsilon^* =$ 3.0, the resulting MD data in the PS fluid exhibit a reasonable agreement with the CS equation in Eq. (3), whereas, with increasing densities, the CS result in the HS fluid strongly overestimates the MD values in the PS fluid at the same density. In the case of ε^* = 3.0, particle penetrability effects start to play a relevant role even in the low density regime. Under these conditions, more particles are forced to overlap as the density increases, resulting in a substantial decrease in the pressure relative to that of the HS system at the same density. Also shown in Fig. 2(a) is the polynomial fitting equation for the PS fluid in Eq. (7). The resulting sets of (c_1, c_2, c_3, c_4) are (0.7246, 0.05757, -0.03788, 0.01132), (2.537, 2.553, -2.842, 1.006), and (2.786, 23.04, -36.26, 15.68) for $\varepsilon^* =$ 0.2, 1.0, and 3.0, respectively. Those empirical data fitting will be useful to regenerate our MD results for the PS compressibility equation for the comparison purpose with relevant theoretical equations.

In the previous theoretical and MC simulation studies of the PS system by Santos and his co-workers,[11] two approximate theories were proposed for the compressibility factor and the contact value of the PS radial distribution function: one valid in the high-penetrability, *i.e.*, small-ε regime, and another in the low-penetrability, *i.e.*, large-ε regime. We will refer to these two theories as the high-penetrability approximation (HPA) and the low-penetrability approximation (LPA), respectively. The detailed expressions for both HPA and LPA equations are available elsewhere.[20] In a given thermodynamic condition of ε^* and φ employed in this work, theoretical predictions for the PS equation of state using HPA and LPA can be evaluated from Eq. (6) together with $g(\sigma^+)$-values listed in the last two columns in Table 1.

In Fig. 2(b), both HPA and LPA approximations for $\varepsilon^* = 0.2$ agree well with MD compressibility data, with the agreement being excellent in the case of the HPA (relative deviations smaller than 0.1%). For $\varepsilon^* = 1.0$, the LPA performs very well, while the HPA is still quite good. It is remarkable that both theories, while being based on opposite approaches, are so close each other up to $\varepsilon^* = 1.0$ and densities as large as $\varphi = 1.0$. For the systems of $\varepsilon^* = 3.0$, the LPA behaves reasonably well up to $\varphi = 0.3$, and the HPA, up to $\varphi = 0.2$. However, the discrepancy for the LPA is gradually amplified with increasing densities, and strongly overestimates the MD values for larger densities. Interestingly enough, the HPA coincidently exhibits a good matching with our MD result for the system of $\varphi = 1.0$ and the least penetrable energy of $\varepsilon^* = 3.0$.

In our MD simulations, as mentioned earlier in this section, we found noticeable differences in the two compressibility expressions in Eqs. (5) and (6) for the systems of $\varphi \geq 0.6$ and $\varepsilon^*=3.0$. A similar behavior was also detected in calculating the contact value of the radial distribution function. According to statistical mechanics, there are two main routes in theoretical and simulation studies to obtain the contact value of the radial distribution function: (i) directly from MC or MD simulation runs and (ii) indirectly from the compressibility equation via the virial route as represented in Eq. (6). In principle, except for unavoidable computational errors, those two methods should generate the same value in equilibrium stable liquid states.

In Fig. 3, we have exhibited the contact value of the PS radial distribution function, $g(\sigma^+)$, obtained from the two methods (i) and (ii). In this figure, the solid symbol corresponds to the direct method (i), and the open symbol, the indirect method (ii), respectively. The solid line represents the CS value in the HS system as given in Eq. (3). As can be seen in this figure, an excellent agreement between those two methods is observed over the entire density range for $\varepsilon^* = 0.2$, and 1.0. In that case of $\varepsilon^* = 3.0$, we observe that, up to $\varphi = 0.2$ the MD values are very close to the HS contact values obtained from the CS formula. This agrees with what is observed in Fig. 2(a) for the HS compressibility factor. Nevertheless, the HS contact values increase rapidly as the density increases, while the PS values reach a maximum around $\varphi = 0.4$ and decrease thereafter. The most striking feature observed in this figure is the separation between the MD values of $g(\sigma^+)$ obtained from methods (i) and (ii) with $\varepsilon^* = 3.0$ and $\varphi \geq 0.6$, with the maximum relative deviation being of almost 30% at $\varphi = 1.0$.

In Fig. 4, we have evaluated the values of the ratio $[g(\sigma^+)/\, g(\sigma^-)]e^{-\varepsilon^*}$ by using the extrapolated MD data of the PS radial distribution function to the contact point. This ratio should take the unity value, except for computational errors, at any given density and repulsive energy parameter if the system is in an equilibrium stable liquid state. We have observed that the deviations from unity are less than 0.1% in the cases of $\varepsilon^* = 0.2$. The internal agreement between $g(\sigma^+)e^{-\varepsilon^*}$ and $g(\sigma^-)$ is also good in the case $\varepsilon^* = 1.0$ with a maximum deviation of about 5% at $\varphi = 0.9$. Again, the least penetrable case of $\varepsilon^* = 3.0$ presents a peculiar behavior. Up to $\varphi = 0.5$ the ratio $[g(\sigma^+)/\, g(\sigma^-)]e^{-\varepsilon^*}$ deviates from unity less than 8%, but thereafter it markedly increases with density until having $[g(\sigma^+)/\, g(\sigma^-)]e^{-\varepsilon^*} \cong 1.6$ at $\varphi = 1.0$. Consequently, this leads to the mismatching of the compressibility data between Eqs. (5) and (6). Such discrepancies, when $\varepsilon^* = 3.0$ and $\varphi \geq 0.6$, are likely due to the appearance of cluster-forming structures in the PS system,[1,4] implicitly indicating that the configurational states reached in our MD simulations are not of strict thermodynamic equilibrium but are long-lived metastable states.

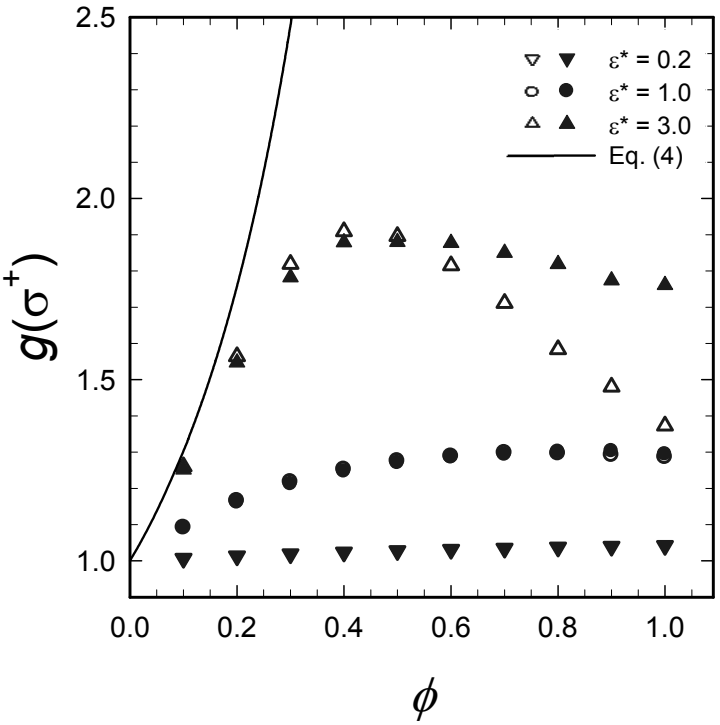

Fig. 3 – The contact value of the radial distribution function as a function of packing fractions for the penetrable-sphere system. The solid and open symbols are obtained directly from the extrapolated MD data of $g(r)$ and indirectly from the virial route in Eq. (6), respectively. The single solid line denotes the Carnahan-Starling prediction in Eq. (4) for the hard-sphere fluid.

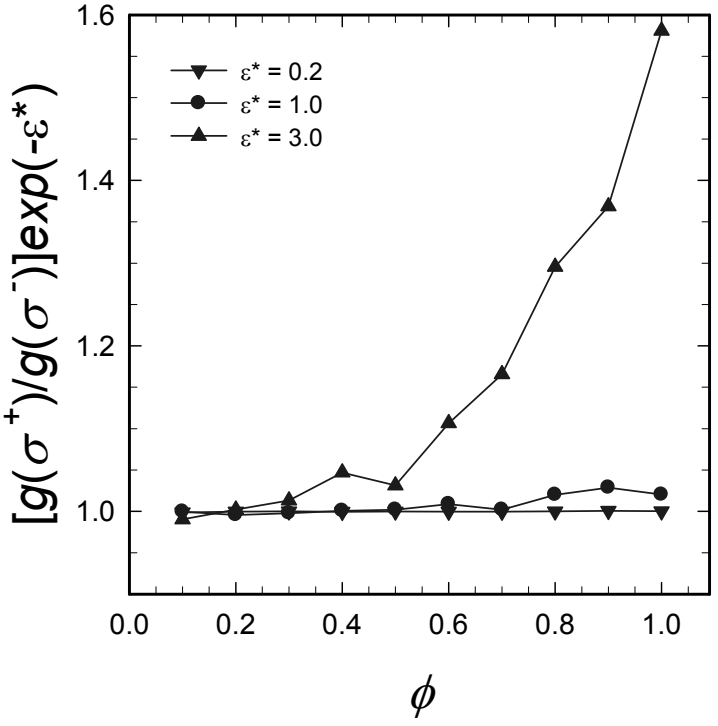

Fig. 4 – The ratio of $[g(\sigma^+)/ g(\sigma^-)]e^{-\varepsilon^*}$ by using the extrapolated MD data of $g(r)$ as a function of packing fractions for the penetrable-sphere system. The lines between symbols are only guide to the eyes.

CONCLUSIONS

In the present work, as an intermediate between theory and experiment, computer simulations via the molecular dynamics method have been carried out to investigate the thermodynamic and structural properties of penetrable-sphere interaction systems over the wide ranges of the packing fraction, φ, and the repulsive energy parameter, ε. The resulting MD simulation data for the configurational energy, the compressibility factor and the contact value of the radial distribution function are used to assess the applicabilities of various theoretical predictions available in the literature including high- and low-penetrability approximations. A reasonable agreement between theoretical and simulation results is found in the cases of low and moderately repulsive systems ($\varepsilon/kT \leq 1.0$). However, for the dense systems of $\varphi \geq 0.6$ with the highly repulsive energy barrier of $\varepsilon/kT = 3.0$, a poor agreement is observed due to the metastable static effects of cluster-forming structures in the phase transition state. Under these conditions the development of cluster formation significantly influences the static equilibrium properties as detected in the discrepancies between the direct MD values and the indirect virial route for the contact value of the radial distribution function. In addition to the static equilibrium properties of the PS fluid observed in this work, we are currently examining the density and repulsive energy dependences of time-dependent transport properties for the self-diffusion, the shear viscosity, and the thermal conductivity coefficients.

Acknowledgements: S.-H.S. would like to thank Prof. Andrés Santos for many enlightening discussions on the subject of this paper and other topics, and also his students, Chun-Ho Kim, Jae-Moon Yang and Young-Jin Ha, for their supports during simulation runs. This work has been supported by the Korea/Roumania Mobility Program in the National Research Foundation of Korea.

REFERENCES

1. C. N. Likos, *Phys. Rep.*, **2001**, *348*, 267.
2. C. Marquest and T. A. Witten, *J. Phys. (France)*, **1989**, *50*, 1267.
3. C. N. Likos, M. Watzlawek and H. Löwen, *Phys. Rev. E*, **1998**, *58*, 3135.
4. M. Schmidt, *J. Phys.: Condens. Matter*, **1999**, *11,* 10163.
5. M. J. Fernaud, E. Lomba and L. L. Lee, *J. Chem. Phys.*, **2000**, *112*, 810.
6. M. Schmidt and M. Fuchs, *J. Chem. Phys.*, **2002**, *117*, 6308.
7. N. Choudhury and S. K. Ghosh, *J. Chem. Phys.*, **2003**, *119*, 4827.
8. L. Acedo and A. Santos, *Phys. Lett. A*, **2004**, *323*, 427.
9. Al. Malijevský and A. Santos, *J. Chem. Phys.*, **2006**, *124*, 074508.
10. A. Santos and A. Malijevský, *Phys. Rev. E*, **2007**, 75, 021201; **2007**, *75*, 049901(E).
11. Al. Malijevský, S. B. Yuste and A. Santos, *Phys. Rev. E*, **2007**, *76*, 021504.
12. A. Santos, R. Fantoni and A. Giacometti, *Phys. Rev. E*, **2008**, *77,* 051206.
13. R. Fantoni, A. Giacometti, Al. Malijevský and A. Santos, *J. Chem. Phys.*, **2009**, *131,* 124106.
14. R. Fantoni, A. Giacometti, Al. Malijevský and A. Santos, *J. Chem. Phys.*, **2010**, *133*, 024101.
15. J.-P. Hansen and I. R. McDonald, "Theory of Simple Liquids", Academic Press, Amsterdam, 2006.
16. M. P. Allen and D. J. Tildesley, "Computer Simulation of Liquids", Clarendon, Oxford Univ. Press, 1987.
17. S.-C. Kim and S.-H. Suh, *J. Chem. Phys.*, **2002**, *117*, 9880.
18. S. Zhou and E. Ruckenstein, *J. Chem. Phys.*, **2000**, *112*, 8079.
19. S.-C. Kim, B.-S. Seong and S.-H. Suh, *J. Chem. Phys.*, **2009**, *131*, 134701.
20. S.-H. Suh, C.-H. Kim, S.-C. Kim and A. Santos, *Phys. Rev. E*, **2010**, *82,* 051202.
21. S.-H. Suh, J.-W. Park, K.-R. Ha, S.-C. Kim and J.M.D. MacElroy, *Molecular Simulation*, **2001**, *27*, 387.
22. S.-H. Suh, J.-W. Lee, H. Moon and J.M.D. MacElroy, *Adsorption*, **2005**, *11*, 373.
23. B. J. Alder and T. E. Wainwright, *J. Chem. Phys.*, **1959**, *31*, 459.
24. A. Santos, in "Rarefied Gas Dynamics: 24th International Symposium on Rarefied Gas Dynamics", *AIP Conf. Proc.* No. 762, AIP, Melville, NY, 2005, p. 276-281.
25. N. F. Carnahan and K. E. Starling, *J. Chem. Phys.*, **1969**, *51*, 635.